Parametric (quasi-Cherenkov) cooperative radiation produced by electron bunches in natural or photonic crystals

S. V. Anishchenko[1]*, V. G. Baryshevsky[1]†

[1] *Nuclear Problems Institute, Bobruiskaya 11, Minsk 220030, Belarus*

Abstract

We use numerical modeling to study the features of parametric (quasi-Cherenkov) cooperative radiation arising when an electron bunch passes through a crystal (natural or artificial) under the conditions of dynamical diffraction of electromagnetic waves in the presence of shot noise. It is shown that in both Laue and Bragg diffraction cases, parametric radiation consists of two strong pulses: one emitted at small angles with respect to the particle velocity direction and the other emitted at large angles to it. Under Bragg diffraction conditions, the intensity of parametric radiation emitted at small angles to the particle velocity direction reaches saturation at sufficiently smaller number of particles than the intensity of parametric radiation emitted at large angles. Under Laue diffraction conditions, every pulse contains two strong peaks, which are associated with the emission of electromagnetic waves at the front and back ends of the bunch. The presence of noise causes a chaotic signal in the interval between the two peaks.

1 Introduction

The generation of short pulses of electromagnetic radiation is a primary challenge of modern physics. They find applications in studying molecular dynamics in biological objects and charge transfer in nanoelectronic devices, diagnostics of dense plasma and radar detection of fast moving objects.

The advances in the generation of short pulses of electromagnetic radiation in infrared, visible, and ultraviolet ranges of wavelengths are traditionally associated with the development of quantum electronic devices - lasers. Radiation in lasers is generated via induced emission of photons by bound electrons.

Electrovacuum devices, operating in a cooperative regime [1, 2], have recently become considered as an alternative to short-pulse lasers, whose active medium is formed by electrons bound in atoms and molecules. These are free electron lasers, cyclotron-resonance masers, and Cherenkov radiators, whose active medium is formed by electron bunches propagating in complex electrodynamical structures (undulators, corrugated waveguides and others). The feature of the cooperative operation regime lies in the fact that the radiation power scales as the squared number of particles in the bunch. This allows calling this regime "superradiance" by analogy with the phenomenon predicted by Dicke in quantum electronics [1]. It should be noted, that the electrons moving in FELs are initially homogeneously distributed in the phase space. As a result, bremsstrahlung starts

*E–mail: sanishchenko@mail.ru

†E–mail: bar@inp.bsu.by

from sponteneous emission. This is true even if the bunch length is much smaller than the radiation wave length. In contrast to bremsstrahlung, Cherenkov (quasi-Cherenkov) radiation starts from coherent emission when such a short-length bunch is injected into a slow-wave structure, i. e. the radiation power is proportional to the squared number of particles. The question arises whether this dependence holds when the bunch length increases.

This paper considers coperative radiation emitted by electron bunches when charged particles pass through crystals (natural or artificial) under the conditions of dynamical diffraction of elctromagnetic waves. Note that a detailed analysis of the features of spontaneous radiation of electrons passing through crystals in both frequency [3] and time [4] domains has been carried out before. This radiation, emitted at both large and small angles with respect to the direction of electron motion, is called the parametric (quasi-Cherenkov) radiation. The problems of amplification of induced parametric radiation have also been thoroughly studied in the literature [5], and the threshold current densities providing lasing in crystals have been calculated [6].

This paper is arranged as follows: In the beginning, a nonlinear theory of interaction of relativistic charged particles and the electromagnetic field in crystals is set forth, followed by the results of numerical calculations of the parametric radiation pulse. Then, the dependence of the radiation intensity on the electron bunch length and the geometrical parameters of the system is considered. The appendix outlines the algorithm used in the simulation. The feature of the algorithm is that it is based on the particle-in-cell method, which enables studying kinetic phenomena. Let us note that in most of the existing codes (see, e.g. [7, 8]) used for simulating the interaction of charged particles and a synchronous wave, the motion of charged particles is considered within the framework of the hydrodynamic approximation.

2 Nonlinear theory of cooperative radiation

A theoretical analysis of parametric radiation can be performed only by means of a self-consistent solution of a nonlinear set of the Vlasov–Maxwell equations:

$$\frac{\partial f}{\partial t} + \vec{v}\frac{\partial f}{\partial \vec{r}} + q_e(\vec{E} + \vec{v} \times \vec{H})\frac{\partial f}{\partial \vec{p}} = 0, \tag{1}$$

$$\begin{aligned} &\nabla \times \vec{E} = -\frac{1}{c}\frac{\partial \vec{H}}{\partial t}, \\ &\nabla \times \vec{H} = \frac{1}{c}\frac{\partial \vec{D}}{\partial t} + \frac{4\pi}{c}\vec{j},\ \vec{j} = q_e \int \vec{v} f d^3\vec{p}, \\ &\nabla \cdot \vec{D} = 4\pi\rho,\ \rho = q_e \int f d^3\vec{p}, \\ &\nabla \cdot \vec{H} = 0, \end{aligned} \tag{2}$$

describing the electron motion in the electric $\vec{E}$ and magnetic $\vec{H}$ fields. Here $f(\vec{r}, \vec{p}, t)$ is the particle distribution function over the coordinates $\vec{r}$ and momenta $\vec{p}$, while $\vec{j}(\vec{r}, t)$ and $\rho(\vec{r}, t)$ are the current and charge densities, respectively. Since the crystal is a periodic linear medium with frequency dispersion, the Fourier transform of the displacement current $\vec{D}(\vec{r}, \omega)$ relates to the electric field $\vec{E}(\vec{r}, \omega)$ as $D(\vec{r}, \omega) = \big(1 + \chi_0(\omega) + \sum_{\vec{\tau}} 2\chi_{\vec{\tau}}(\omega)\cos(\vec{\tau}\vec{r})\big)\vec{E}(\vec{r}, \omega)$, where the summation is made over all reciprocal lattice vectors. Because the dielectric susceptibilities in natural crystals and in grid photonic crystals are inversely proportional to the frequency [9]: $\chi_{0,\vec{\tau}}(\omega) = \Omega^2_{0,\vec{\tau}}/\omega^2$, Maxwell's equations (2) can be reduced to the equation of the form:

$$\frac{1}{c^2}\frac{\partial^2 \vec{E}}{\partial t^2} + \nabla(\nabla\cdot\vec{E}) - \Delta\vec{E} + \frac{\Omega_0^2}{c^2}\vec{E} + \sum_{\vec{\tau}} 2\frac{\Omega_{\vec{\tau}}^2}{c^2}\cos(\vec{\tau}\vec{r})\vec{E} = -\frac{4\pi}{c^2}\frac{\partial\vec{j}}{\partial t}. \tag{3}$$

We shall further be interested in the case when two strong waves are excited in the crystal: the forward wave and the diffracted wave (the so-called two-wave diffraction case). The forward wave (its wave vector is denoted by $\vec{k}$) is emitted at small angles with respect to the particle velocity, while the diffracted one, having the wave vector $\vec{k}_\tau = \vec{k} + \vec{\tau}$, is emitted at large angles to it (Fig. 1). Under the conditions of dynamical diffraction, the following relation is fulfilled: $\vec{k}_\tau^2 \approx \vec{k}^2 \approx \omega^2/c^2$.

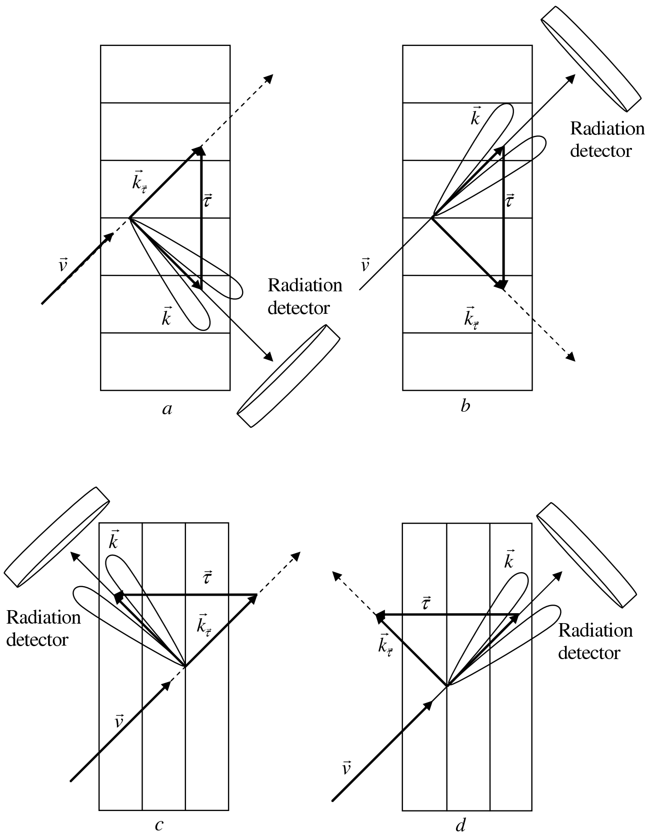

Figure 1: Schemes of parametric radiation in Laue (a, b) and Bragg (c, d) geometries.

Let us perform the following simplifications: First, we shall neglect the longitudinal ($\nabla\cdot\vec{D}\to 0$) fields of the bunch, which is appropriate when the value of the Langmuir oscillation frequency Ω_b of the bunch is less than the values of $\Omega_{0,\tau}$. In this case, the Coulomb forces will not have an appreciable effect on dielectric properties of the system. Second, we shall seek for the electric field $\vec{E}$ using the method of slowly varying amplitudes. Third, we shall assume that a transversally infinite bunch executes one-dimensional motion along the OZ-axis (this is achieved by inducing a strong axial magnetic field in the system).

Under the conditions of two-wave diffraction, the field $\vec{E}$ can be presented as a sum

$$\vec{E} = \vec{e}_0 E_0(z,t) e^{i(\vec{k}\vec{r}-\omega t)} + \vec{e}_\tau E_\tau(z,t) e^{i(\vec{k}_\tau\vec{r}-\omega t)}, \tag{4}$$

where the amplitudes of the forward E_0 and diffracted E_τ waves are slowly varying variables. This means that for the distances comparable with the wavelength and the times comparable with the oscillation period, the values of E_0 and E_τ remain practically the same. Substituting (4) into (1) and (3) and then averaging them over the length $l = 2j\lambda = 2j\pi/k_z$, where j is a natural number, we obtain

$$\frac{\partial f}{\partial t} + v_z \frac{\partial f}{\partial z} + 2q_e \mathrm{Re}\Big(E_0 e^{i(k_z z - \omega t)}\Big) \frac{\partial f}{\partial p_z} = 0, \tag{5}$$

$$\begin{aligned} &\frac{1}{c}\frac{\partial E_0}{\partial t} + \gamma_0 \frac{\partial E_0}{\partial z} + \frac{i\Omega_0^2}{2\omega c} E_0 + \frac{i\Omega_\tau^2}{2\omega c} E_\tau = -\frac{2\pi}{c}\int_{z-l/2}^{z+l/2} e_{0z} j_z e^{i(\omega t - k_z z)} dz/l, \gamma_0 = k_z/k, \\ &\frac{1}{c}\frac{\partial E_\tau}{\partial t} + \gamma_\tau \frac{\partial E_\tau}{\partial z} + \frac{i\Omega_0^2}{2\omega c} E_\tau + \frac{i\Omega_\tau^2}{2\omega c} E_0 = -\frac{2\pi}{c}\int_{z-l/2}^{z+l/2} e_{\tau z} j_z e^{i(\omega t - k_{\tau z} z)} dz/l, \gamma_\tau = k_{\tau z}/k. \end{aligned} \tag{6}$$

Now let us complete the set of equations (5) and (6) with boundary conditions (the initial conditions are reduced to the condition that all values of the fields equal zero at $t = 0$): in the plane $z = 0$, let us specify the time dependence of function f and set the field E_0 to zero. In the case of Bragg diffraction, the boundary condition imposed on the diffracted wave is reduced to the condition that the field E_τ equals zero at $z = L$, while in the case of Laue diffraction, it equals zero at $z = 0$.

The difference between the two diffraction schemes is not merely kinematic, but radical. Under Bragg diffraction conditions, there is a synchronous wave moving against the electrons of the beam, which gives rise to the internal feedback and absolute instability. In Laue diffraction geometry, a backward wave is absent, and as a result absolute instability does not evolve. It may seem that electromagnetic radiation is not generated. However, fluctuations, which always occur in real beams, are amplified when the beam enters the crystal (due to convective instability, excited in the beam).

In analyzing multiparametric problems, to which the problem of parametric cooperative radiation refers, it is convenient to write equations (5) and (6) in a dimensionless form. This procedure enabled transferring the calculation results from one set of wavelengths and beam energies to another. The analysis shows that this procedure is easy to perform in the case when the electrons of the beam are ultrarelativistic (the Lorentz factor $\gamma \gg 1$).

Let us note that the kinetic equation (1) is equivalent to the system of relativistic equations of motion for the momenta $\vec{p}_j$ and coordinates $\vec{r}_j$ of particles, since

$$f = \sum_j \delta(\vec{r} - \vec{r}_j)\delta(\vec{p} - \vec{p}_j)$$

(the lower index j runs over all beam's electrons inside the crystal). When $\gamma \gg 1$, these equations are convenient to write with the phases of charged particles $\phi_j = \vec{k}_0\vec{r}_j - \omega t$ substituted for independent variables. The substitution of variables $\omega t\theta^2 \to t$, $\omega L\theta^2/c \to L$, $mc\omega\theta E_{0,\tau}/q_e \to E_{0,\tau}$ (θ is the angle between the particle velocity and the wave vector $\vec{k}$) then gives

$$\frac{d^2\phi_j}{dt^2} = 2\Big(-2\frac{d\phi_j}{dt} - 1\Big)^{3/2} \mathrm{Re}\Big(E_0 e^{i\phi_j}\Big), \tag{7}$$

$$\begin{aligned} &\frac{\partial E_0}{\partial t} + \gamma_0 \frac{\partial E_0}{\partial z} + \frac{i\chi_0}{2\theta^2} E_0 + \frac{i\chi_\tau}{2\theta^2} E_\tau = -\sum_j \frac{\chi_{bj}}{2\theta^2}\frac{e^{-i\phi_j}}{N_l}, \\ &\frac{\partial E_\tau}{\partial t} + \gamma_\tau \frac{\partial E_\tau}{\partial z} + \frac{i\chi_0}{2\theta^2} E_\tau + \frac{i\chi_\tau}{2\theta^2} E_0 = 0. \end{aligned} \tag{8}$$

Here the quantity $\chi_{bj} = -4\pi q_e^2 n_j/m\omega^2$ is determined at the moment when the jth particle enters the system, n_j is the corresponding electron density, and N_l is the number of particles over the length l. The set of equations with boundary conditions contains four independent parameters: $\chi_{0,\tau,b}/\theta^2$, $\omega L\theta^2/c$ that define the geometry of the system. In addition to these parameters, we need to specify the beam profile. Let

$$\chi_b = \chi_{b0}(1 - e^{-ct/L_f})e^{\Theta(ct-L_b)(ct-L_b)/L_f}, \tag{9}$$

where the rise time L_f/c is further assumed to be equal to $0.1L_b/c$ (L_b is the bunch length and Θ is the Heaviside function).

3 Simulation results

The characteristic feature of cooperative pulses is the peculiar dependence of the peak power on the number of particles N_b in the bunch. When the particles are small in number, the radiation power monotonically increases until saturation is achieved.

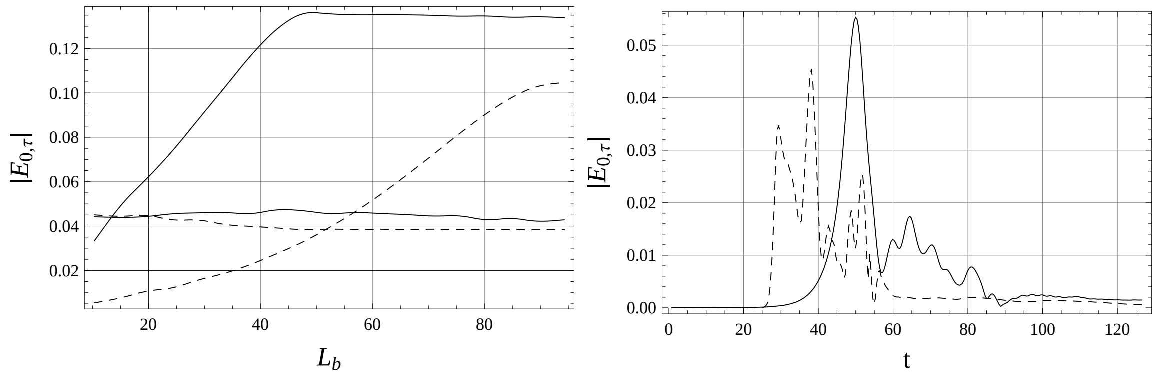

Figure 2: Parametric radiation under Bragg diffraction conditions. Left: peak values of the fields $|E_{0,\tau}|$ plotted as a function of the bunch length. Two upper curves are plotted for radiation at large angels, while the two lower ones - for radiation at small angles. Solid curves illustrate the case when $\gamma_\tau = -1$; dashed curve - the case when $\gamma_\tau = -0.5$. Right: the example of a cooperative pulse $[\gamma_\tau = -1.0]$. Solid curve refers to a diffracted wave, dashed curve – to a direct one.

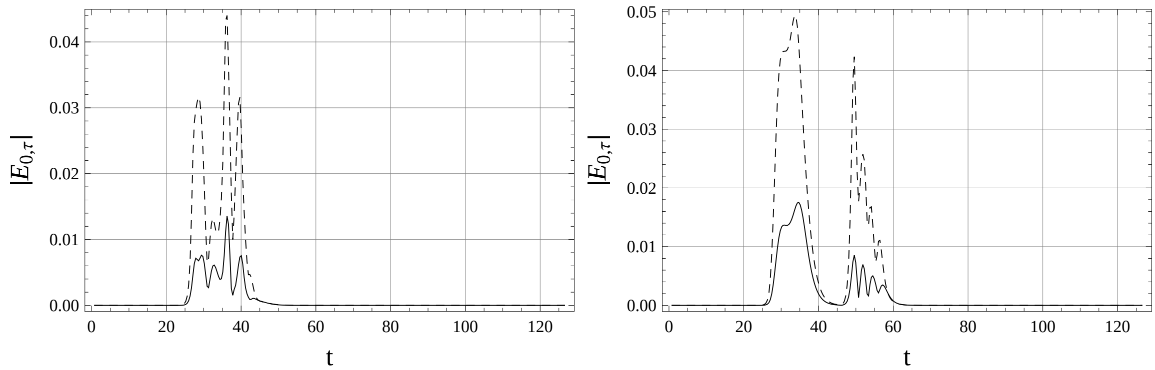

Figure 3: Parametric radiation under Laue diffraction conditions. Solid curve is plotted for radiation at large angels, while dashed curve – for radiation at small angles. $[\gamma_\tau = -0.5]$. Left plot: $L_b = 12.4$. Right plot: $L_b = 24.9$.

Let us see now how the dynamical diffraction of electromagnetic waves affects the cooperative radiation in crystals. Does parametric radiation possess the above described

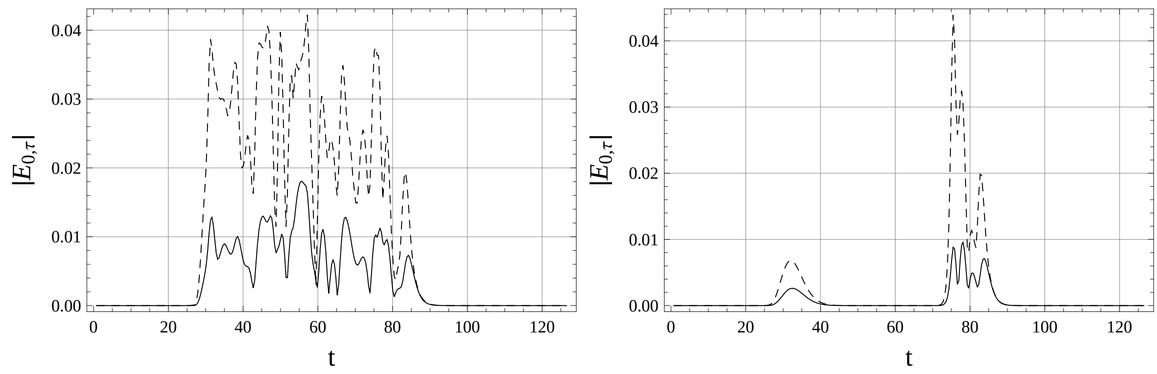

Figure 4: Pulse of cooperative radiation under Laue diffraction conditions in the presence of noise (left) and without it (right). Solid curve shows radiation at large angles, dashed curve - radiation at small angles. The amplitude of white noise ratio to the average current density is assumed to be $j_{rand0}/j_{av} = 0.01$. Computation is made for the case when the bunch length $L_b = 49.8$.

features inherent to other types of cooperative radiation? How the Bragg diffraction case is different from the case of Laue diffraction?

We shall assume that $\gamma = 5$, $\chi_0 = \chi_\tau = 0.06$, $\gamma_0 = 0.98$ and specify the system of units, where $c = 1$, $\omega\theta^2 = 1$, $mc\omega\theta/q_e = 1$ and $L = 24.9$.

Let us start our consideration with Bragg diffraction. The results of computation (Fig. 2) show that the radiation emitted at small angles reaches saturation at significantly smaller lengths of the bunch than that emitted at large angles. The transition from a one-dimensional distributed feedback ($\gamma_\tau = -1$) to a two-dimensional one ($\gamma_\tau \neq -1$) hardly causes any change in the intensity of radiation emitted at small angles to the particle velocity.

Under Laue diffraction conditions, the pulse of parametric radiation has a more complicated structure due to the convective character of instability: in the absence of noise, the generation occurs only at the ends of the bunch of charged particles. As a result, the cooperative pulse possess a two-peak structure (Fig. 3). The presence of noise leads to an appreciable change in the pulse form: the interval between the two pulses is filled with a chaotic signal (Fig.4).

4 Conclusion

This paper studies the features of parametric cooperative radiation emitted at both large and small angles to the particle velocity direction. Both Laue and Bragg cases are considered. It is shown that under Bragg diffraction conditions, the intensity of parametric radiation emitted at small angles reaches saturation at significantly smaller number of particles in the bunch than the intensity of radiation emitted at large angles.

Under Laue diffraction conditions, the pulses of parametric radiation, emitted at both large and small angles to the particle velocity, possess a two-peak structure; each of the peaks is associated with the front or back end of the bunch. The presence of noise leads to an appreciable change in the pulse form: the interval between the two pulses is filled with a chaotic signal.

A Particle-in-cell method

The set of equations (5) and (6) was solved using the particle-in-cell method, which is widely used in plasma physics [10, 11]. This method implies that the solution of the kinetic equation is modeled using a large number of macroparticles moving along the characteristics of the kinetic equation. The current and charge densities are calculated from particle velocities and positions and are further used for computations of the electric field on a space-time mesh. The mesh values of the field are interpolated to the macroparticle locations; then the forces acting on macroparticles are calculated. The approach described here is close to the method described by I. J. Morey and C. K. Birdsall in [12], which was used for travelling wave tube modeling.

Let us introduce a spatial $\omega_z = \{z_n = n\Delta z, n = 0, 1, ..., n_{max}, n_{max}\Delta z = L\}$ and a time $\omega_t = \{t_s = s\Delta t, s = 0, 1, ...\}$ mesh. Specify an implicit finite-difference scheme of field equations (6) with second order accuracy in time and coordinate:

$$
\begin{aligned}
&\text{at } n = 0: \ E_{0n}^{s+1} = 0,\\
&\frac{E_{\tau n}^{s+1} - E_{\tau n}^{s}}{c\Delta t} = -\gamma_\tau \frac{-3E_{\tau n}^{s+1/2} + 4E_{\tau n+1}^{s+1/2} - E_{\tau n+2}^{s+1/2}}{2\Delta z} - \frac{i\chi_0}{2}E_{\tau n}^{s+1/2} - \frac{i\chi_\tau}{2}E_{0n}^{s+1/2},\\
&\text{at } n = n_{max}: \ E_{\tau n}^{s+1} = 0,\\
&\frac{E_{0n}^{s+1} - E_{0n}^{s}}{c\Delta t} = -\gamma_0 \frac{3E_{0n}^{s+1/2} - 4E_{0n-1}^{s+1/2} + E_{0n-2}^{s+1/2}}{2\Delta z} - \frac{i\chi_0}{2}E_{0n}^{s+1/2} - \frac{i\chi_\tau}{2}E_{\tau n}^{s+1/2} - J_{0n}^{s+1/2},\\
&\text{at } 0 < n < n_{max}:\\
&\frac{E_{0n}^{s+1} - E_{0n}^{s}}{c\Delta t} = -\gamma_0 \frac{E_{0n+1}^{s+1/2} - E_{0n-1}^{s+1/2}}{2\Delta z} - \frac{i\chi_0}{2}E_{0n}^{s+1/2} - \frac{i\chi_\tau}{2}E_{\tau n}^{s+1/2} - J_{0n}^{s+1/2},\\
&\frac{E_{\tau n}^{s+1} - E_{\tau n}^{s}}{c\Delta t} = -\gamma_\tau \frac{E_{\tau n+1}^{s+1/2} - E_{\tau n-1}^{s+1/2}}{2\Delta z} - \frac{i\chi_0}{2}E_{\tau n}^{s+1/2} - \frac{i\chi_\tau}{2}E_{0n}^{s+1/2}.
\end{aligned}
\tag{10}
$$

Let us define the source $J_{0n}^{s+1/2}$ on the right-hand side of (10), using the formula

$$
\begin{aligned}
J_{0n}^{s+1/2} = \frac{2\pi \sin\theta e^{i\omega(t+\Delta t/2)}}{cl} \Big(&\sum_j Q_j v_{zj}^{s+1/2} \frac{z_{n+1} - z_j^{s+1/2}}{\Delta z} e^{-ik_z z_j^{s+1/2}}\\
&+ \sum_j Q_j v_{zj}^{s+1/2} \frac{z_j^{s+1/2} - z_{n-1}}{\Delta z} e^{-ik_z z_j^{s+1/2}} \Big).
\end{aligned}
\tag{11}
$$

The contributions to each node come from the particles concentrated in the domain $z_{n-1} \leq z_j < z_{n+1}$. Summation in the first and second terms is made over all particles in the domains $z_n \leq z_j^{s+1/2} < z_{n+1}$ and $z_{n-1} \leq z_j^{s+1/2} < z_n$, respectively. The weighting factors $\frac{z_{n+1}-z_j^{s+1/2}}{\Delta z}$ and $\frac{z_j^{s+1/2}-z_{n-1}}{\Delta z}$ are responsible for linear interpolation of the contributions to the node with number n that come from each particle.

Complete the implicit difference scheme (10) with the discrete analogues of the equations of motion of macroparticles:

$$
\begin{aligned}
&\frac{p_{zj}^{s+1} - p_{zj}^{s}}{\Delta t} = 2Q_j \mathrm{Re}\big(E_{0j}^{s+1/2} e^{ik_z z_j^{s+1/2} - i\omega(t+dt/2)}\big), p_j^{s+1/2} = \frac{p_j^{s+1} + p_j^{s}}{2},\\
&\frac{z_j^{s+1} - z_j^{s}}{\Delta t} = v_{zj}^{s+1/2}, v_{zj}^{s+1/2} = \frac{p_{zj}^{s+1/2}/M_j}{\sqrt{1 + (p_{zj}^{s+1/2}/M_j c)^2}}.
\end{aligned}
\tag{12}
$$

The field $E_j^{s+1/2}$ at particles' locations can be found by means of linear interpolation from surrounding nodes:

$$E_{0j}^{s+1/2} = \frac{z_{n+1} - z_j^{s+1/2}}{\Delta z} E_{0n}^{s+1/2} + \frac{z_j^{s+1/2} - z_n}{\Delta z} E_{0n+1}^{s+1/2}, \quad z_n \leq z_j^{s+1/2} < z_{n+1}. \tag{13}$$

Injection and extraction of particles are performed as follows: during every time step, we inject ΔN number of particles, whose coordinates are

$$z = -\Delta z\left(1 + \frac{i}{\Delta N}\right), i = 0, 1, ..., \Delta N - 1.$$

Assume that each particle has a momentum p_{z0} and a charge $Q = j_{av}\Delta t + j_{rand}\Delta t$. Here j_{av} is the average current density and j_{rand} is a random quantity. This quantity appears due to shot noise of charged particles, which in high power devices can achieve quite large values, because the electron flow consists of ectons [13]. Since the parametric radiation is narrow-band by nature, and the current density spectrum j_{rand} is a slowly varying function of frequency ω, one can replace the real current density j_{rand} by a random quantity uniformly distributed in the domain $(-j_{rand0}, j_{rand0})$. The level of noise is determined by the fluctuation current density $j_{rand0}(\omega)$. By analogy with the case of fluctuations of current, particle distribution over momenta can be introduced into the system. Particles are extracted from the system after they reach the coordinate $z_j \geq L + \Delta z$.

References

[1] R. Bonifacio, et. al. Rivista Nuovo Cimento. 1990. Vol. 13. No. 9. P. 1.

[2] S. D. Korovin, et. al. Phys. Rev. E. 2006. Vol. 74. P. 016501.

[3] V. G. Baryshevsky, I. D. Feranchuk, and A. P. Ulyanenkov, *Parametric X-Ray Radiation in Crystals: Theory, Experiment and Applications*, Springer-Verlag, Berlin Heidelberg, 2005.

[4] S. V.Anishchenko, V. G. Baryshevsky, and A. A. Gurinovich. NIM B. 2012. Vol. 293. P. 35.

[5] V. G. Baryshevsky, I. D. Feranchuk. Phys. Lett. A. 1984. Vol. 102. P. 141.

[6] V. G. Baryshevsky, arXiv: 1211.4769 (2012).

[7] T. M. Antonsen, et. al. Proceedings of the IEEE. Vol. 87. (1999) 804.

[8] N. S. Ginzburg, S. P. Kuznecov, T. H. Fedoseeva. Izv. vuzov. Radiofizika. Vol. 21. P. 1037.

[9] V. G. Baryshevsky, A. A. Gurinovich. NIM B. 2006. Vol. 252. P. 92.

[10] J. P. Verboncoeur. Plasma Phys. Control. Fusion. 2005. Vol. 47. P. A231.

[11] A. G. Sveshnikov, S. A. Jakunin. Matem. Model. 1989. Vol. 1. No. 4. P. 1.

[12] I. J. Morey, C. K. Birdsall. Memorandum No. UCB/ERL M89/116. Electronics Research Laboratory. University of California. 1989.

[13] E. B. Abubakirov, A. P. Konjushkov, A. S. Sergeev. Radiotehnika i electronika. 2009. Vol. 54. P. 1009.